

# Ground-State Ordering of the $J_1$ – $J_2$ Model on the Simple Cubic and Body-Centered Cubic Lattices

D. J. J. Farnell

*School of Dentistry, Cardiff University,  
Cardiff CF14 4XY, Wales, United Kingdom*

O. Götze and J. Richter

*Institut für Theoretische Physik, Universität Magdeburg, D-39016 Magdeburg, Germany*

(Dated: June 2, 2016)

## Abstract

The  $J_1$ – $J_2$  Heisenberg model is a “canonical” model in the field of quantum magnetism in order to study the interplay between frustration and quantum fluctuations as well as quantum phase transitions driven by frustration. Here we apply the Coupled Cluster Method (CCM) to study the spin-half  $J_1$ – $J_2$  model with antiferromagnetic nearest-neighbor bonds  $J_1 > 0$  and next-nearest-neighbor bonds  $J_2 > 0$  for the simple cubic (SC) and body-centered cubic (BCC) lattices. In particular, we wish to study the ground-state ordering of these systems as a function of the frustration parameter  $p = z_2 J_2 / z_1 J_1$ , where  $z_1$  ( $z_2$ ) is the number of nearest (next-nearest) neighbors. We wish to determine the positions of the phase transitions using the CCM and we aim to resolve the nature of the phase transition points. We consider the ground-state energy, order parameters, spin-spin correlation functions as well as the spin stiffness in order to determine the ground-state phase diagrams of these models. We find a direct first-order phase transition at a value of  $p = 0.528$  from a state of nearest-neighbor Néel order to next-nearest-neighbor Néel order for the BCC lattice. For the SC lattice the situation is more subtle. CCM results for the energy, the order parameter, the spin-spin correlation functions and the spin stiffness indicate that there is no direct first-order transition between ground-state phases with magnetic long-range order, rather it is more likely that two phases with antiferromagnetic long-range are separated by a narrow region of a spin-liquid like quantum phase around  $p = 0.55$ . Thus the strong frustration present in the  $J_1$ – $J_2$  Heisenberg model on the SC lattice may open a window for an unconventional quantum ground state in this three-dimensional spin model.

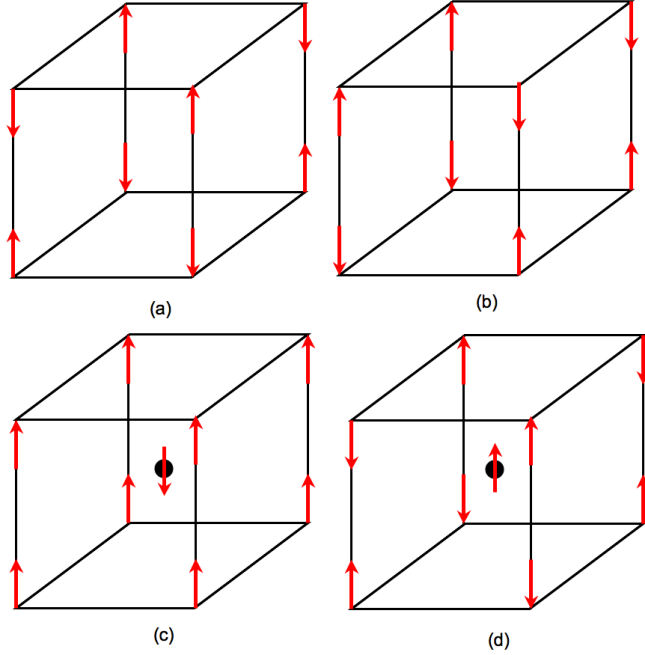


FIG. 1: CCM model states: (a) Néel model state for the simple cubic lattice (denoted by SC-AF1); (b) striped model state for the simple cubic lattice (denoted by SC-AF2); (c) nearest-neighbor Néel model state for the body-centered cubic lattice (denoted by BCC-AF1); (d) next-nearest-neighbor Néel striped model state for the body-centered cubic lattice (denoted by BCC-AF2).

## I. INTRODUCTION

Frustrated quantum magnetism continues to attract enormous attention both in theory and experiment[1–3]. A canonical model to study the interplay of frustration and quantum fluctuations is the spin-half  $J_1$ – $J_2$  Heisenberg model. On the square lattice this model has been extensively utilized to study frustration-driven quantum phase transitions between semiclassical ground-state phases with magnetic long-range order and magnetically disordered quantum phases, see, e.g., Refs. [4–30]. Despite of the numerous investigations of the two-dimensional (2D) model the nature of the non-magnetic quantum phase around  $J_2/J_1 = 0.5$  is still under debate. Interest in the spin-half  $J_1$ – $J_2$  model on square lattice is motivated also by its relation to experimental studies of various magnetic materials, such as  $\text{VOMoO}_4$  (Ref. [31]),  $\text{Li}_2\text{VO SiO}_4$ , and  $\text{Li}_2\text{VO GeO}_4$  (Ref. [32]) or  $\text{Sr}_2\text{CuTeO}_6$  (Ref. [33]).

The dimension of the underlying lattice is crucial to the existence of magnetic long-range order in quantum magnetic systems. Naturally there is a stronger tendency to order in

three-dimensional (3D) systems. Thus, already a quite small coupling between the  $J_1 - J_2$  square-lattice layers leads to a disappearance of the magnetically disordered phase [34–37]. However, a magnetically disordered quantum phase is not per se excluded in frustrated 3D systems, as it has been demonstrated for the spin-half Heisenberg antiferromagnet (HAFM) on the pyrochlore lattice [38].

The natural 3D counterpart of the square-lattice  $J_1$ - $J_2$  model is the  $J_1$ - $J_2$  model on the body-centered cubic (BCC) lattice. The limiting case of  $J_1 = 0$  and  $J_2 > 0$  belongs to the case of two interpenetrating unfrustrated, i.e. bipartite, antiferromagnets for both models. The few investigations of the 3D BCC spin-half  $J_1$ - $J_2$  model include exact diagonalization (ED) [39], series expansions around the Ising limit [40], spin-wave theory [39, 41], and the random phase approximation [42]. Thus, all methods (except ED) start from the symmetry-broken classical antiferromagnetic states and then quantum corrections are subsequently taken into account. Consistently, all of these methods indicate that a single phase transition occurs in this system. In contrast to the 2D model, a magnetically disordered quantum phase is not observed. However, the frustration has a strong influence on the thermodynamics, in particular the critical temperature is substantially suppressed by frustration [40, 43–45].

Less clear is the situation for the spin-half  $J_1$ - $J_2$  model on the simple cubic (SC) lattice [43, 46–52]. In this case different approaches, such as, spin-wave theories [46–48, 51], variational cluster approach [52], differential operator technique [50] or a spherically symmetric Green function method [49], come to different conclusions with respect to the existence of a disordered ground-state phase. The underlying semi-classical physics of these approaches is different. Spin-wave theories [46–48, 51], differential operator technique [50], and the variational cluster approach [52] include explicit symmetry breaking. Spin-wave theory uses the  $z$ -axis aligned classical states as a starting point for the calculation, whereas differential operator technique and the variational cluster approach use Weiss fields to test the presence of the antiferromagnetic order. By contrast, the Green function method [49] preserves full spin rotational invariance. A direct first-order transition between two antiferromagnetically long-range ordered phases was obtained in Refs. [46, 48, 50, 51], whereas within Green function technique [49] and linear spin-wave theory [51] a magnetically disordered quantum phase was found that separates the two antiferromagnetic phases. Very recently the role of a third-neighbor coupling,  $J_3$ , was studied by Laubach et al. [52]. Although, these authors did not discuss a disordered quantum phase for  $J_3 = 0$ , their results indicate that a very small

additional frustrating  $J_3 > 0$  leads to such a spin-liquid like quantum phase. It is in order to emphasize the basic difference between the BCC and SC  $J_1$ - $J_2$  models, that becomes evident in the limit of large  $J_2$  (or  $J_1 \rightarrow 0$ ). Contrary to the BCC model, the  $J_1$ - $J_2$  HAFM on the SC model is still strongly frustrated, because the antiferromagnetic  $J_2$  bonds connect sites of two interpenetrating face-centered cubic (FCC) lattices.

In the present paper we use the coupled cluster method (CCM) to perform a comparative study of the spin-half  $J_1$ - $J_2$  HAFM on the BCC and SC lattices. We mention here, that the CCM previously has been applied to the 2D square-lattice  $J_1$ - $J_2$  HAFM [10, 14, 16, 17, 26, 53] and the method provides accurate results for the ground-state energy, the magnetic order parameter as well as for the critical points, where the quantum phase transitions take place.

The relevant Hamiltonian of the  $J_1$ - $J_2$  model is given by

$$H = J_1 \sum_{\langle i,j \rangle} \mathbf{s}_i \cdot \mathbf{s}_j + J_2 \sum_{\langle\langle i,j \rangle\rangle} \mathbf{s}_i \cdot \mathbf{s}_j . \quad (1)$$

The symbol  $\langle i,j \rangle$  indicates those bonds that connect nearest-neighbor sites (counting each bond once only) and the symbol  $\langle\langle i,j \rangle\rangle$  indicates those bonds that connect next-nearest-neighbor sites (again counting each bond once only). Here we consider the SC and BCC lattices in the regime  $J_1 \geq 0$  and  $J_2 \geq 0$ , and these lattices (and CCM “model states”, see Sec. II) are shown in Fig. 1. We note that these systems are frustrated by positive values of  $J_2$ . The competition between the bonds  $J_1$  and  $J_2$  and therefore the phase transition points in these systems depend on coordination numbers  $z_1$  (i.e., the number of nearest-neighbors) and  $z_2$  (i.e., the number of next-nearest-neighbors). In order to enable our calculations to be consistent with each other, we introduce the following quantity,

$$p = \frac{J_2 z_2}{J_1 z_1} . \quad (2)$$

The (underlying) BCC and SC lattices are both bipartite, and so the nearest-neighbor Néel state forms the classical ground state for both of these systems for smaller values of  $p < p_{\text{cl}}$ , i.e., up to the phase transition point at  $p = p_{\text{cl}}$ , where  $p_{\text{cl}} = \frac{1}{2}$  for the SC as well as for the BCC lattice. These states are shown in Fig. 1 for both the SC and BCC lattices. They are denoted by SC-AF1 and BCC-AF1, respectively. The situation is more complicated in the large  $p$  limit. The BCC lattice decouples into two SC lattices when nearest-neighbor bonds are set to  $J_1 = 0$  and  $J_2$  remains non-zero. Thus, collinear striped order (the corresponding state is denoted by BCC-AF2) occurs for  $p > p_{\text{cl}}$  for the BCC

lattice, also shown in Fig. 1 for the BCC lattice. We shall use this state as another model state for the BCC lattice. By contrast, the SC lattice decouples into two FCC lattices when nearest-neighbor bonds are set to  $J_1 = 0$  and  $J_2$  remains non-zero. This system (with only next-nearest-neighbor antiferromagnetic bonds) is therefore frustrated and there is a highly degenerate classical ground-state manifold including non-collinear ground states. However, according to the *order by disorder* mechanism [54, 55] collinear striped ordering is favored by quantum fluctuations [46–52] also for  $p > p_{cl}$ . The “striped” model state for the SC lattice (denoted by SC-AF2) used here is also shown in Fig. 1.

Here we wish to investigate the ground-state properties of the spin-half  $J_1$ – $J_2$  model on the SC and BCC lattices by using the CCM. We wish to determine the positions of the phase transitions using the CCM and we aim to discuss the nature of the phase transitions. As there is arguably less evidence available in the literature for the SC lattice rather than the BCC lattice, this investigation should be most useful for the SC lattice. However, we shall see that insight into both systems can be obtained by comparing and contrasting the results for each system.

In what follows, the formalism of the CCM is presented briefly, and then the results for the BCC lattice and the SC lattice are given. We present our conclusions in the final section of this paper.

## II. METHOD

For general information relating to the methodology of the CCM, see, e.g., Refs. [56–60]. The CCM has recently been applied computationally at high orders of approximation to quantum magnetic systems with much success, see, e.g., Refs. [61–72]. In the field of quantum magnetism, advantages of this approach are that it can be applied to strongly frustrated quantum spin systems in any dimension and with arbitrary spin quantum numbers. The exact ket and bra ground-state energy eigenvectors,  $|\Psi\rangle$  and  $\langle\tilde{\Psi}|$ , of a many-body system described by a Hamiltonian  $H$ ,

$$H|\Psi\rangle = E_g|\Psi\rangle ; \quad \langle\tilde{\Psi}|H = E_g\langle\tilde{\Psi}| , \quad (3)$$

are parametrized within the CCM as follows:

$$|\Psi\rangle = e^S|\Phi\rangle ; \quad S = \sum_{I \neq 0} \mathcal{S}_I C_I^+ ,$$

$$\langle \tilde{\Psi} | = \langle \Phi | \tilde{S} e^{-S} \quad ; \quad \tilde{S} = 1 + \sum_{I \neq 0} \tilde{\mathcal{S}}_I C_I^- . \quad (4)$$

Again, we remark that the model or reference states  $|\Phi\rangle$  for the SC and BCC lattices are shown in Fig. 1. The ground-state energy is now given by

$$E_g = E_g(\{\mathcal{S}_I\}) = \langle \Phi | e^{-S} H e^S | \Phi \rangle . \quad (5)$$

The ket-state and bra-state correlation coefficients are obtained by solving the CCM ket- and bra-state equations given by

$$\langle \Phi | C_I^- e^{-S} H e^S | \Phi \rangle = 0, \quad \forall I \neq 0, \quad (6)$$

$$\langle \Phi | \tilde{S} e^{-S} [H, C_I^+] e^S | \Phi \rangle = 0, \quad \forall I \neq 0. \quad (7)$$

Each ket- or bra-state equation belongs to a certain creation operator  $C_I^+ = s_i^+, s_i^+ s_j^+, s_i^+ s_j^+ s_k^+, \dots$ , i.e. it corresponds to a certain set (configuration or cluster) of lattice sites  $i, j, k, \dots$ . The ket- and bra-state correlation coefficients  $\mathcal{S}_I$  and  $\tilde{\mathcal{S}}_I$ , respectively, relate to the “fundamental” cluster with index  $I$  (of  $N_f$  such fundamental clusters in total) and so also to the appropriate ground-state equation above.

The manner in which the CCM equations are determined and solved is discussed elsewhere (again, see, e.g., Refs. [61–72] for more details). However, it is important to note here that the CCM formalism is only ever exact in the limit of inclusion of all possible multi-spin cluster correlations within  $S$  and  $\tilde{S}$ , although in any real application this is usually impossible to achieve. It is therefore necessary to utilize various approximation schemes within  $S$  and  $\tilde{S}$ . The most commonly employed scheme has been the localized LSUB $m$  scheme, in which all multi-spin correlations over distinct locales on the lattice defined by  $m$  or fewer contiguous sites are retained. We will use this scheme in this article.

Note that we also make the specific and explicit restriction that the creation operators  $\{C_I^+\}$  in  $S$  preserve the relationship that, in the original (unrotated) spin coordinates,  $s_T^z = \sum_i s_i^z = 0$  in order to keep the approximate CCM ground-state wave function in the correct ( $s_T^z = 0$ ) subspace. Note that each fundamental cluster is independent of all others clusters with respect to the symmetries of the lattice (and Hamiltonian).

The order parameter (sublattice magnetization)  $M$  for the systems considered here is defined as

$$M = -\frac{1}{N} \sum_i^N \langle \tilde{\Psi} | \hat{s}_i^z | \Psi \rangle , \quad (8)$$

where we note that  $\hat{s}_i^z$  is with respect to the local spin axes at site  $i$  *after rotation* of the local spin axes with respect to the model state so that (*notationally only*) the spins appear to align in the negative  $z$ -direction. This ensures that the mathematics of treating these problems is slightly simpler [60, 61]. Hence, the order parameters are taken with respect to the model states shown in Fig. 1.

As mentioned above, the LSUB $m$  approximation becomes exact only in the limit  $m \rightarrow \infty$ , and so it is useful to extrapolate the LSUB $m$  results in this limit. A well-established extrapolation scheme [60–72] for the ground-state energy,  $E_g/N$ , is given by

$$e_g(m) = E_g(m)/N = e_g(m = \infty) + a_1 m^{-2} + a_2 m^{-4}. \quad (9)$$

For the magnetic order parameter  $M$  we use the scheme

$$M(m) = M(m = \infty) + b_1/m^{1/2} + b_2/m^{3/2}. \quad (10)$$

This extrapolation ansatz is most suitable to detect ground-state order-disorder transitions [16, 17, 26, 64–67]. We were able to carry out CCM calculations to the LSUB8 level of approximation for the BCC lattice and to LSUB10 for the SC lattice. The maximum number of fundamental configurations entering the CCM calculations at the LSUB10 level of approximation is 1,728,469.

We know from Refs. [16, 17, 26, 64–67] that the lowest level of approximation, LSUB2, conforms poorly to the extrapolation schemes, especially as the parameter  $p$  increases. Hence, as in previous calculations, we exclude LSUB2 data from the extrapolations.

Specifically for the SC lattice we will also calculate the spin stiffness  $\rho$  up to the LSUB8 level of approximation. More explanation is needed relating to how to define the stiffness and how to perform the necessary CCM calculations, and so we transfer this discussion to the Appendix A.

### III. RESULTS

#### A. Body-Centered Cubic Lattice

The BCC lattice is considered firstly. We were able to carry out CCM calculations to the LSUB8 level of approximation for this system. Results for the ground-state energy are shown

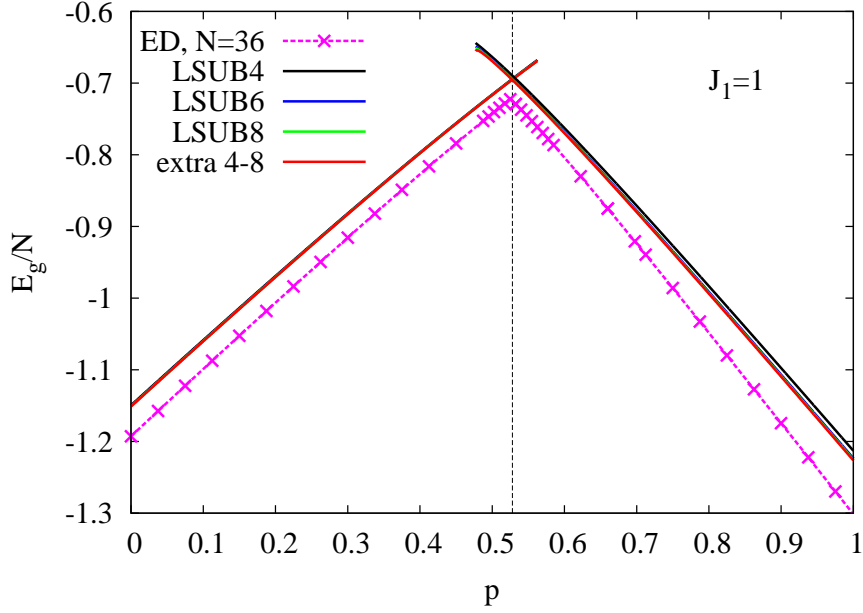


FIG. 2: CCM results for the ground-state energy of the spin-half  $J_1$ - $J_2$  model on the BCC lattice are compared to results of exact diagonalizations (ED) with  $N = 36$ . Note that the curves for the LSUB $m$  data coincide almost completely. Extrapolated results (label ‘extra 4-8’) are obtained by using the extrapolation scheme of Eq. (9) using data from the LSUB4, LSUB6, and LSUB8 approximations. The ground-state energies of the two model states are found to intersect at  $p_c = 0.528$ .

in Fig. 2. LSUB $m$  results converge very rapidly with increasing level of approximation  $m$ , and differences in energies between LSUB6 and LSUB8 levels of approximation are broadly of order  $10^{-4}$  for the BCC-AF1 model state and of order  $10^{-3}$  for the BCC-AF2 model state and for all values of  $p$ . LSUB4, LSUB6, and LSUB8 results for the unfrustrated case where  $p = 0$  (setting also  $J_1 = 1$ ) are given by  $e_g = -1.14950$ ,  $-1.15072$ , and  $-1.15101$ , respectively. The extrapolation to  $m = \infty$  yields  $e_g = -1.1513$ , which compares well to results of series expansions of  $e_g = -1.1510$  [74] and of third-order spin-wave theory of  $e_g = -1.1512$  [74]. Good correspondence with ED results of Ref. [39] are also seen by visual inspection of Fig. 2. We observe that CCM and ED results follow a very similar pattern as we increase  $p$ , although ED results are clearly much lower in energy than those of the CCM. The difference between ED and CCM results is due to the finite size of the lattice ( $N = 36$ ) in the ED calculations. The overall behavior of the ground-state energy provides



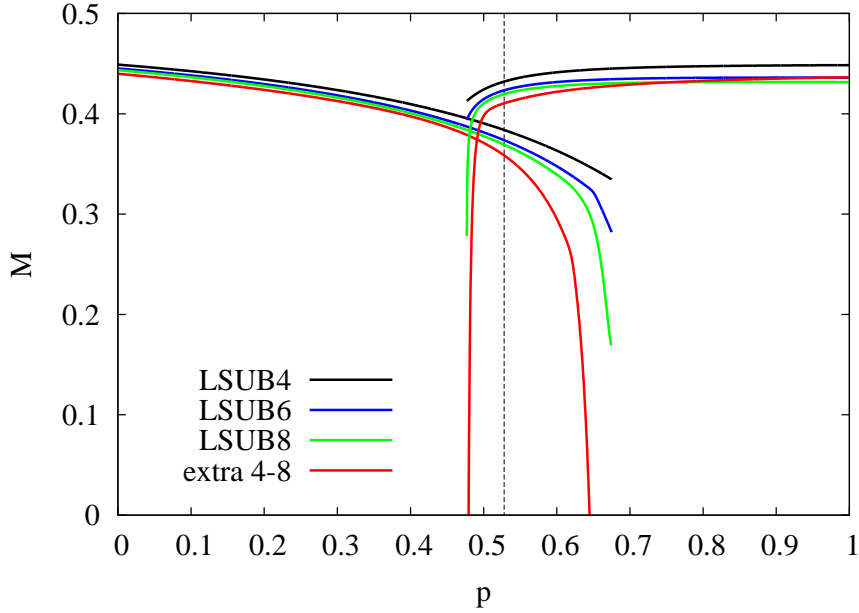


FIG. 3: CCM results for the order parameter (sublattice magnetization)  $M$  of the spin-half  $J_1$ – $J_2$  model on the BCC lattice. Extrapolated results (label ‘extra 4-8’) are obtained by using the extrapolation scheme of Eq. (10) using data from the LSUB4, LSUB6, and LSUB8 approximations. The vertical (dotted) line indicates the intersection point of the ground-state energies for the two model states at  $p_c = 0.528$ .

clear evidence for a first-order transition. The intersection point at  $p = p_c = 0.528$  of the ground-state energies of the BCC-AF1 and BCC-AF2 energies determines the transition point. The corresponding kink in the  $e_g(p)$ -curve for  $N = 36$  (ED) is at  $p \approx 0.525$ .

Results for the order parameter are shown in Fig. 3. We see again that CCM results are converging with increasing level of LSUB $m$  approximation level, albeit more slowly than for the ground-state energy. LSUB4, LSUB6, and LSUB8 results for the unfrustrated HAFM (i.e., when  $p = 0$ ) are given by  $M = 0.44899$ ,  $0.44515$ , and  $0.44350$  respectively, and the extrapolated value is  $M = 0.4398$ . Again, this result compares quite well to those predictions of series expansions of  $M = 0.442$  [74] and of third-order spin-wave theory of  $M = 0.4412$  [74]. The data shown in Fig. 3 clearly support that there is a direct first-order transition between the phases with semi-classical magnetic long-range orders of type AF1 and AF2 (see Fig. 1). The values of the extrapolated order parameter at the transition point  $p_c = 0.528$  are  $M = 0.3585$  (AF1) and  $M = 0.4104$  (AF2).

The results for the spin-spin correlation functions at the LSUB8 level of approximation

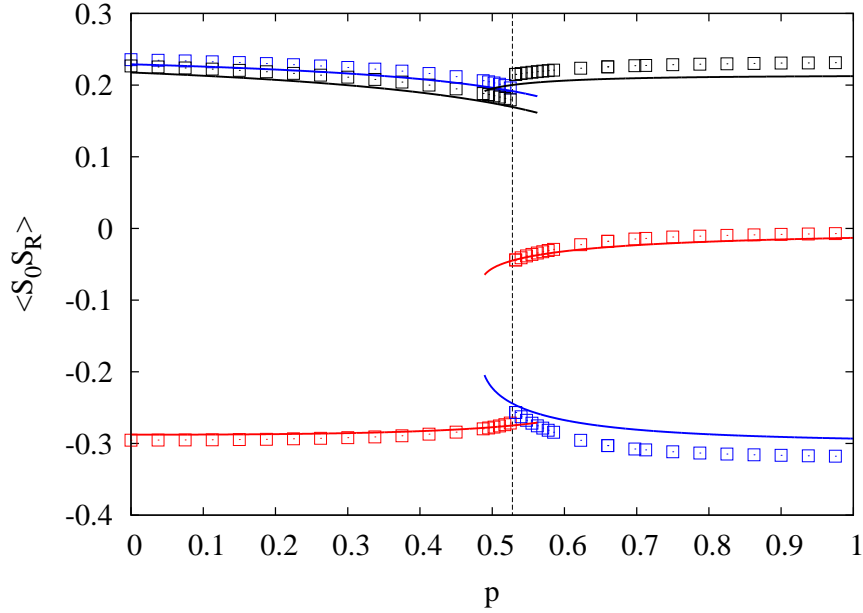


FIG. 4: Spin-spin correlation  $\langle \mathbf{S}_0 \mathbf{S}_{\mathbf{R}} \rangle$  functions for nearest neighbors (red), next-nearest neighbors (blue) and for third-nearest neighbors (black) for the spin-half  $J_1$ - $J_2$  model on the BCC lattice in dependence of the frustration parameter  $p = 3J_2/4J_1$  (solid lines - CCM-LSUB8 results, symbols - ED results for  $N = 36$ , cf. Ref. [39]). All results are averaged data over all neighbors with the same separation  $|\mathbf{R}|$ .

shown in Fig. 4 agree well with the ED data for  $N = 36$ . The change in the spin-spin correlation functions is very abrupt and the large magnitude of correlation functions at  $p = p_c$  is a further evidence of a first-order phase transition at this point. The small magnitude of the nearest-neighbor spin-spin correlation function at  $p > p_c$  signals the splitting of the system in two weakly coupled interpenetrating antiferromagnets with leading coupling  $J_2$ .

We may compare the transition point  $p_c = 0.528$  obtained by the CCM with previous results, namely  $p_c = 0.525$  (ED [39]),  $p_c \approx 0.53$  (series expansions [40] and non-linear spin-wave theory [41]),  $p_c \approx 0.54$  (random phase approximation[42]). Note that the critical point for the quantum model is slightly above the classical value  $p_{cl} = 0.5$ .

Finally, we emphasize the basic difference to the 2D square-lattice model (see also the discussion in the next section). Although, both models are of similar character concerning the competition between the  $J_1$  and  $J_2$  bonds, the increase in dimension leads to a significant stabilization of semi-classical magnetic long-range order and to the disappearance of the intermediate quantum phase that is present in the 2D model. Thus, the amount of frustration

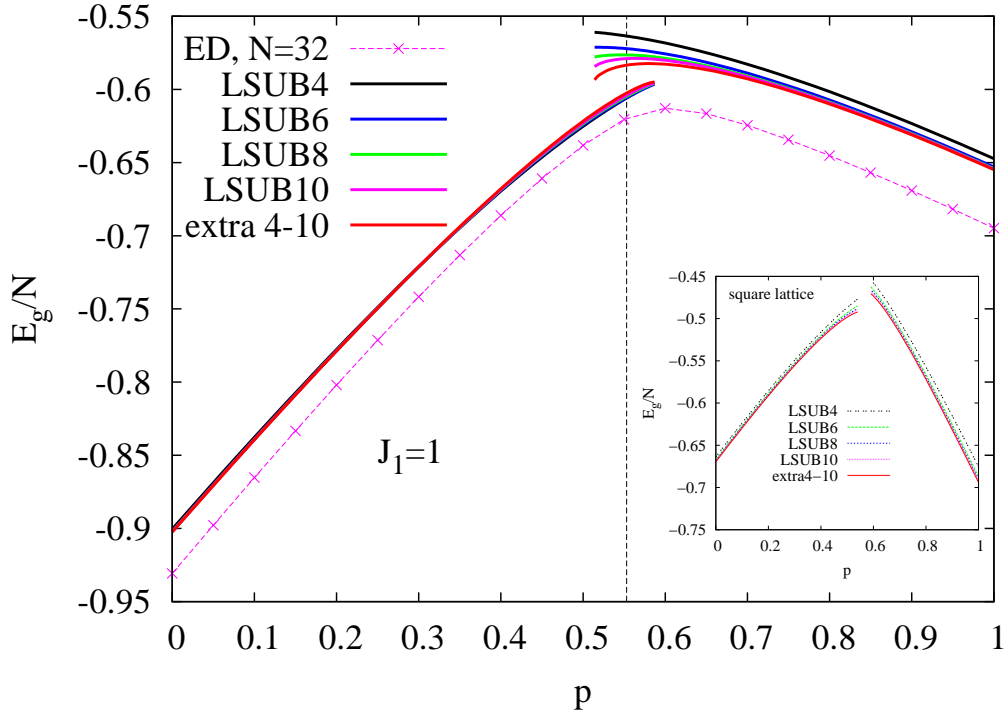


FIG. 5: CCM results for the ground-state energy  $E_g/N$  for the spin-half  $J_1$ - $J_2$  model on the SC lattice are compared to results of exact diagonalizations (ED) with  $N = 32$ . Note that the curves for the LSUB $m$  data obtained for the Néel model state coincide almost completely. Extrapolated results (label ‘extra 4-10’) are obtained by using the extrapolation scheme of Eq. (9) using data from the LSUB4, LSUB6, LSUB8, and LSUB10 approximations. The vertical (dotted) line indicates the value in the middle of the two points,  $p_c^{AF1} = 0.549$  and  $p_c^{AF2} = 0.557$ , where the extrapolated order parameters of the SC-AF1 and SC-AF2 phases vanish. (Inset: CCM results for the spin-half square-lattice  $J_1$ - $J_2$  model corresponding to Ref. [17].)

must be larger in 3D for such a magnetically disordered quantum phase to exist at all. The  $J_1$ - $J_2$  model on the SC lattice discussed in the next section might have a sufficient degree of frustration because the next-nearest-neighbor bonds  $J_2$  in this model compete not only with the nearest-neighbor bonds  $J_1$  but also with each other.

## B. Simple Cubic Lattice

Next we consider the SC lattice. We were able to carry out CCM calculations to the LSUB10 level of approximation for this system. Results for the ground-state energy on the

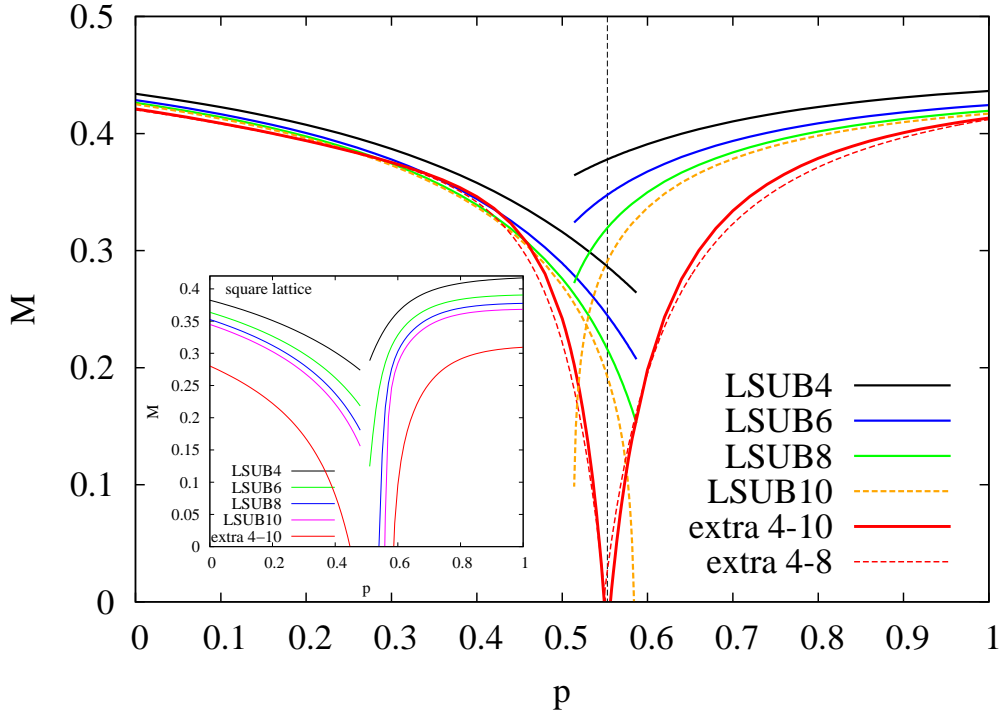


FIG. 6: CCM results for the order parameter (sublattice magnetization)  $M$  of the spin-half  $J_1$ - $J_2$  model on the SC lattice. Extrapolated results are obtained by using the scheme of Eq. (10). To get an impression of the accuracy of the extrapolated order parameter we take into account (i) data from the LSUB4, LSUB6, LSUB8, and LSUB10 approximations (thick solid red line, label ‘extra 4-10’) and (ii) data from the LSUB4, LSUB6, and LSUB8 approximations (thin dotted red line, label ‘extra 4-8’). Obviously, both red lines are very close to each other. The vertical (dotted) line indicates the value in the middle of the two phase transition points  $p_c^{AF1} = 0.549$  and  $p_c^{AF2} = 0.557$ . (Inset: CCM results for the spin-half square-lattice  $J_1$ - $J_2$  model corresponding to Ref. [17].)

SC lattice are shown in Fig. 5. LSUB $m$  results are essentially converged at the LSUB10 level of approximation for the Néel model state SC-AF1 (differences in energy between the LSUB8 and LSUB10 levels of approximation are generally much less than  $10^{-3}$  for all values of  $p$ .) Results for the striped model state SC-AF2 (only) do not demonstrate quite the same level of convergence as those results for the SC-AF1 Néel model state, although they are still close to each other. For the unfrustrated SC HAFM (i.e., when  $p = 0$  and setting also  $J_1 = 1$ ) LSUB4, LSUB6, LSUB8, and LSUB10 results are  $e_g = -0.90043$ ,  $-0.90180$ ,  $-0.90214$ , and  $-0.90225$ , respectively. We find an extrapolated CCM result of  $e_g = -0.9024$

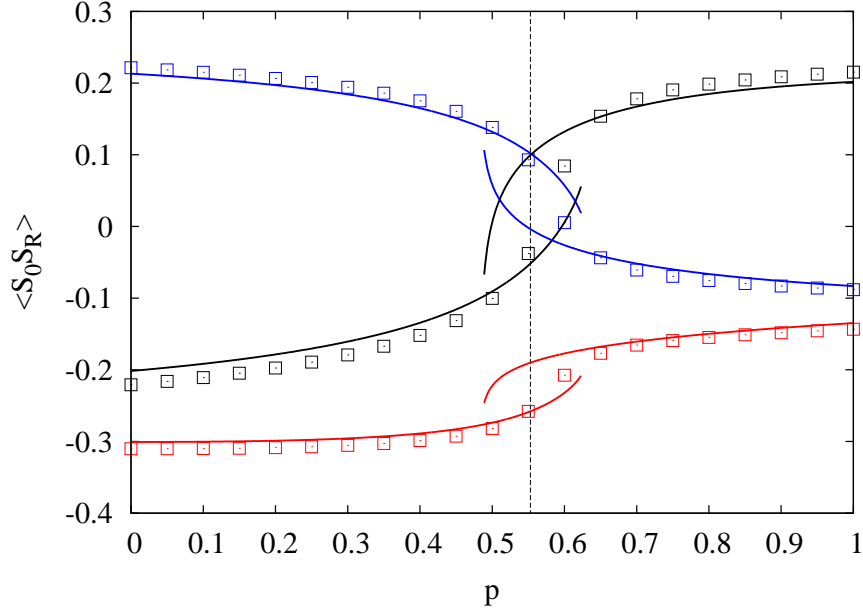


FIG. 7: Spin-spin correlation  $\langle \mathbf{S}_0 \mathbf{S}_{\mathbf{R}} \rangle$  functions for nearest neighbors (red), next-nearest neighbors (blue) and for third-nearest neighbors (black) for the spin-half  $J_1$ - $J_2$  model on the SC lattice in dependence of the frustration parameter  $p = 3J_2/4J_1$  (solid lines - CCM-LSUB8 results, symbols - ED results for  $N = 32$ ). All results are averaged data over all neighbors with the same separation  $|\mathbf{R}|$ .

which compares well to results of series expansions of  $e_g = -0.9021$  [74] and of third-order spin-wave theory of  $e_g = -0.9025$  [74]. Good correspondence with ED results is again seen by visual inspection of Fig. 5, although the difference between ED and CCM results is again due to the finite size of the lattice ( $N = 32$ ) in the ED calculations.

The curvature of the  $e_g(p)$  curve around  $p = 0.55$  is noticeably different to the results for the ground-state energy for the BCC lattice near to its transition point. Moreover, we find that the solution to the LSUB10 equations on the SC lattice terminates at  $p \sim 0.58$  for the SC-AF1 model state tracing and at  $p \sim 0.52$  for the SC-AF2 model state (i.e., we cannot trace the CCM solution beyond these termination points). One may expect that any intersection should occur within the region  $0.52 \lesssim p \lesssim 0.58$ , see Fig.5. However, a (tentative) extension of the ground-state energy for SC-AF1 model state beyond  $p \sim 0.58$  with respect to  $p$  until it crosses those results for the SC-AF1 model state leads to a speculative crossing point at  $p \approx 0.65$ , which is therefore clearly too large. We mention again that the energies for the Néel and striped model states demonstrate a very clearly defined intersection at  $p_c$

for the BCC case, see Fig.2. On the other hand, the behavior of the ground-state energy of the spin-half square-lattice  $J_1$ - $J_2$  model, as is shown by the inset to Fig. 5, is quite similar to that of the SC lattice.

Results for the order parameter  $M$  are shown in Fig. 6. We see again that CCM results converge with increasing level of LSUB $m$  approximation level. In order to provide an idea of the precision of the extrapolation of the order parameter according to Eq. (10) two extrapolation schemes are presented in Fig. 6 : (i) data from the LSUB4, LSUB6, LSUB8, and LSUB10 approximations are used for the extrapolation and (ii) only data from the LSUB4, LSUB6, and LSUB8 approximations are used. The results obtained by scheme (i) should be regarded as more accurate than scheme (ii) because it contains more data to extrapolate with and higher orders of approximation. However, the differences in extrapolated results between both schemes remain small in the entire parameter region. LSUB2, LSUB4, LSUB6, LSUB8, and LSUB10 results for the unfrustrated HAFM (i.e. when  $p = 0$ ) are  $M = 0.45024$ ,  $0.43392$ ,  $0.42860$ ,  $0.42626$ , and  $0.42504$ , respectively. We find an extrapolated CCM result of  $M = 0.4210$  ( $M = 0.4164$ ) for scheme (i) [scheme (ii)], and this result compares reasonably well to results of series expansions of  $M = 0.424$  [74] and of third-order spin-wave theory of  $M = 0.4227$  [74].

A striking difference to the BCC case is shown by the critical points that are estimated by finding the values at which the extrapolated order parameter becomes zero. We find  $p_c^{AF1} = 0.549$  and  $p_c^{AF2} = 0.557$  for scheme (i), whereas we have  $p_c^{AF1} = 0.551$  and  $p_c^{AF2} = 0.548$  for scheme (ii). Again, results of scheme (i) ought to be more accurate than those of scheme (ii), although the agreement between both schemes is a good check of the consistency of our results. We conclude that the spin-half  $J_1$ - $J_2$  HAFM on the SC lattice possesses an intermediate quantum phase between two semi-classical magnetic phases with continuous transitions between the phases. Again, this behaviour is highly reminiscent of the behaviour for the order parameter of the spin-half square-lattice  $J_1$ - $J_2$  model, as is shown by the inset to Fig. 6. However, the intermediate quantum paramagnetic regime is much clearer for this 2D model. Thus, our data obtained by a high-order CCM approximation provide serious indications, but not definite evidence, for the presence of the intermediate quantum phase for the SC lattice.

Results for the spin-spin correlation functions are shown in Fig. 7, where CCM results are again in good agreement with results of ED ( $N = 32$ ). The overall shape of the correlation

functions around  $p = 0.55$  is in accordance with a continuous transition. Their behavior is quite different to the results for the BCC model. For example, results for the nearest-neighbor and next-nearest-neighbor correlation functions demonstrate a large discontinuity in values in the region of transition (centered on  $p_c \approx 0.53$ ) for the BCC lattice, as shown in Fig. 4. By contrast, the changes in the spin-spin correlation functions for the SC lattice near the phase transition points are clearly of smaller magnitude and are much smoother than for the BCC lattice, as shown in Fig. 7 for both the ED and CCM results.

In addition to the sublattice magnetization  $M$  we can also use the spin stiffness  $\rho_s$  (see App. A) to get an independent analysis of order-disorder quantum phase transitions. A positive value of  $\rho_s$  means that there is magnetic long-range order in the system, whereas a value of zero reveals that there is no magnetic long-range order. Results for  $\rho_s$  of the spin-half  $J_1$ - $J_2$  model on the SC lattice are given in Fig. 8. For the unfrustrated SC Heisenberg antiferromagnet, i.e. at the point  $p = 0$ , we found  $\rho_s^{AF1} = 0.24158, 0.23803, 0.23654$  at the LSUB4, LSUB6, and LSUB8 levels of approximation. (Note that the LSUB4 and LSUB6 data coincide with those of Ref. [75], whereas the LSUB8 result is new). The extrapolated result is  $\rho_s^{AF1}(p = 0) = 0.2332$ , that is close to the result of Ref. [75] obtained without LSUB8. We also mention that the CCM value  $\rho_s^{AF1}(p = 0) = 0.2332$  is in very good agreement with  $\rho_s^{AF1}(p = 0) = 0.2343$  obtained by second-order spin-wave theory [76].

At small values of  $p$  the stiffness  $\rho_s^{AF1}$  decreases linearly with increasing  $p$ . That is similar to the classical result  $\rho_{s,cl}^{AF1}(p) = \rho_{s,cl}^{AF1}(p = 0) - bp$ , however with a reduced slope of  $b = 0.43$  instead of  $b = 0.5$ . Approaching the transition point  $p_c$  we find a slight upturn in  $\rho_s^{AF1}$ , and, as a result, we cannot determine a transition point by  $\rho_s^{AF1}$ . We argue, that likely higher orders of LSUB $m$  approximations are required to overcome this problem. However, we may speculate that the linear relation  $\rho_s^{AF1}(p)$  (valid at small  $p$ ) remains approximately valid until  $p_c$ . A corresponding extrapolation (see the dashed magenta line in Fig. 8) crosses the  $x$ -axis at  $p = 0.540$ , i.e. close to the  $p_c$  value found from the order parameter  $M$ , see Fig. 6.

In the AF2 phase at larger values of the frustration parameter  $p$  the stiffness  $\rho_s^{AF2}(p)$  behaves quite differently. Asymptotically it saturates as  $p \rightarrow \infty$  (note that  $\rho_{s,cl}^{AF2}(p) = \text{const.}$ ). As approaching  $p_c$  from the right,  $\rho_s^{AF2}(p)$  drops down and the stiffness extrapolated according to Eq. (A2) vanishes at  $p = 0.540$ , i.e. at that value, where the linear fit of  $\rho_s^{AF1}(p)$  becomes zero. We remark that  $\rho_s^{AF2}$  and the linear fit of  $\rho_s^{AF1}(p)$  both tend to zero at a value of  $p$  that is consistent with results for the vanishing points of the order parameter  $M$

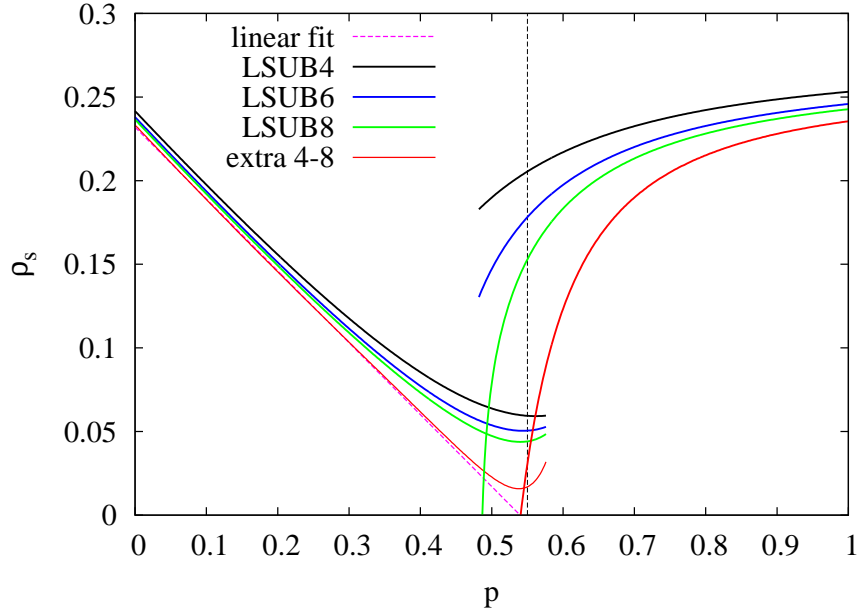


FIG. 8: CCM results for the spin stiffness for the spin-half  $J_1$ - $J_2$  model on the SC lattice. Extrapolated results (label ‘extra 4-8’) are obtained by using the extrapolation scheme of Eq. (A2) using data from the LSUB4, LSUB6, and LSUB8 approximations. For the classical model we have  $\rho_{s,cl}^{AF1} = s^2 (J_1 - 4J_2)$  and  $\rho_{s,cl}^{AF2} = s^2 J_1$ .

using model states AF1 and AF2. All of these results demonstrate that the transition is different to that for the BCC lattice. Furthermore, the behavior of the ground-state energy, the order parameter, and the stiffness are quite similar to that found for the square-lattice  $J_1$ - $J_2$  HAFM [17], albeit with an intermediate quantum phase that is much smaller for the 3D SC lattice.

#### IV. CONCLUSIONS

The ground-state phases of the spin-half  $J_1$ - $J_2$  HAFM on the BCC and SC lattices were investigated by using the CCM in this article. Two antiferromagnetic regimes of collinear order were observed for the BCC lattice, namely, of nearest-neighbor Néel and next-nearest-neighbor Néel striped long-range order. An intersection point between the ground-state energies for these two model states was observed at  $p = 0.528$  [where  $p = (z_2 J_2)/(z_1 J_1)$ ], and no intermediate magnetically disordered phase was detected. The gradient of the ground-state energy with respect to  $p$  (and also for the spin-spin correlation functions using ED)



behaved discontinuously at the intersection point. The values for the corresponding order parameters at this point are  $M \sim 0.36 \sim 0.41$ . These results are all clear indications of a single first-order phase transition occurring at  $p \sim 0.53$ , which is in agreement with results of all other approximate methods [39–42] applied to this model.

The spin-half  $J_1$ – $J_2$  HAFM on the SC lattice is more strongly frustrated due to the self-frustrating character of the  $J_2$  bonds. Although the data for the SC lattice were harder to resolve, our results demonstrate that the ground-state phase diagram is very different to that of the BCC lattice. In particular, the investigation of the magnetic order parameter indicates that there is an intermediate quantum phase in between the two semi-classical magnetic phases. Thus, the phase diagram of the spin-half  $J_1$ – $J_2$  HAFM on the SC lattice resembles that of the corresponding 2D model. Trivially, any investigation of a highly non-trivial quantum many-body system relies on approximations. Bearing in mind that we find a very small parameter region where this quantum phase may exist, we cannot exclude that the actual phase diagram does not exhibit such a quantum phase. However, our data provide evidence that the quantum  $J_1$ – $J_2$  model on the SC lattice is a candidate for a 3D spin system, where strong frustration may lead to a non-magnetic quantum ground state. Moreover, any additional competing term in the Hamiltonian would further open the window for an unconventional quantum phase.

Evidence in the literature relating to the existence of the intermediate quantum phase for the SC lattice is mixed, and certainly there is no consensus as to its nature, if indeed it does exist. However, there are some similarities between the behavior of the  $J_1$ – $J_2$  model on the SC lattice and that of the square-lattice  $J_1$ – $J_2$  model. It is worth noting that calculations for the square-lattice model using density matrix renormalization group with explicit implementation of SU(2) spin rotation symmetry in Ref. [24] have found a gapless spin liquid for  $0.44 < J_2/J_1 < 0.5$  and a gapped plaquette valence-bond phase for  $0.5 < J_2/J_1 < 0.61$ . However, any inference relating to the ground-state ordering of the SC-lattice model in the intermediate regime based on the behavior of the square-lattice model would be highly speculative. Bearing in mind that the region of a possible intermediate phase is very small, it seems that the emergence of a sizable gap in this phase is unlikely, i.e., we may expect that the intermediate phase is either a gapless spin liquid or a phase with a very small gap, cf. also the discussion in Ref. [52].

## Appendix A: The spin stiffness of the SC $J_1$ - $J_2$ antiferromagnet

The spin stiffness  $\rho_s$  measures the increase in the amount of energy as we twist the magnetic order parameter of a magnetically long-range ordered system along a given direction by a small angle  $\theta$  per unit length, see, e.g., Refs. [72, 77–80]. We use here the notations given in Ref. [79] and define the stiffness tensor as

$$\rho^{\alpha\beta} = \left. \frac{\partial^2 e_g(\mathbf{Q})}{\partial \theta_\alpha \partial \theta_\beta} \right|_{\mathbf{Q}=0}, \quad (\text{A1})$$

where  $e_g = E_g/N$  is the ground-state energy per spin,  $\theta_\alpha = \mathbf{Q} \cdot \mathbf{e}_\alpha$  ( $\alpha = 1, 2, 3$ ) are the twist angles along the basis vectors  $\mathbf{e}_\alpha$ , and  $\mathbf{Q}$  is the magnetic wave vector of the magnetically long-range ordered phase.

For the SC lattice we have trivially  $\mathbf{e}_\alpha = \mathbf{e}_{x,y,z}$ . The corresponding magnetic wave-vectors are  $\mathbf{Q} = (\pi, \pi, \pi)$  for the AF1 (Néel) state (see Fig. 1a) and  $\mathbf{Q} = (\pi, 0, \pi)$  for the AF2 (striped) state (see Fig. 1b). For the classical model in the AF1 phase we easily obtain  $\rho_{cl}^{\alpha\beta} = \rho_{s,cl}^{AF1} \delta_{\alpha\beta}$  with  $\rho_{s,cl}^{AF1} = s^2 (J_1 - 4J_2)$ , i.e. the stiffness tensor is diagonal and naturally the  $x$ ,  $y$  and  $z$ -components are identical.

For the magnetic wave vector  $\mathbf{Q} = (\pi, 0, \pi)$  (AF2 state) we have to consider the twists  $\theta_\alpha = \mathbf{Q} \cdot \mathbf{e}_\alpha$ , i.e.  $\theta_x = \theta_1$ ,  $\theta_y = 0$ ,  $\theta_z = \theta_2$ , and we obtain for the classical model again a diagonal tensor  $\rho_{cl}^{\alpha\beta} = \rho_{s,cl}^{AF2} \delta_{\alpha\beta}$  with  $\rho_{s,cl}^{AF2} = s^2 J_1$ . The CCM calculation for the quantum  $s = 1/2$  model is straightforward, see Refs. [17, 72, 75, 80]. We introduce the twist as described above and use the twisted state as the model state for the CCM calculation. As a result we obtain the quantum ground-state energy as a function of the imposed twist angle that can be used to find  $\rho_s^{AF1}$  and  $\rho_s^{AF2}$  according to Eq. (A1). However, note that the solution of the corresponding CCM-LSUB $m$  equations is more challenging because fewer point-group symmetries can be used for the non-collinear twisted state and so we have more fundamental clusters at equivalent level of LSUB $m$  approximation. Therefore we can only calculate the stiffness only up to LSUB8. We follow Refs. [17, 72, 75, 80] and extrapolate the stiffness CCM-LSUB $m$  data to  $m \rightarrow \infty$  using LSUB4, LSUB6 and LSUB8 data by using the extrapolation scheme given by

$$\rho_s(m) = \rho_s(m = \infty) + c_1 m^{-1} + c_2 m^{-2}. \quad (\text{A2})$$

- 
- [1] J. Richter, J. Schulenburg and A. Honecker, in *Quantum Magnetism*, Lecture Notes in Physics Vol. 645, ed. U. Schollwöck, J. Richter, D. J. J. Farnell and R. F. Bishop (Springer-Verlag, Berlin, 2004), pp. 85-153.
  - [2] *Introduction to Frustrated Magnetism. Materials, Experiments, Theory*, ed. C. Lacroix, P. Mendels and F. Mila (Springer-Verlag, Berlin, Heidelberg, 2011).
  - [3] L. Balents, *Nature* **464**, 199 (2010).
  - [4] C. L. Henley and S. Prakash, *J. de Physique Colloq.* **49**, C8-1197 (1988); C. L. Henley, *Phys. Rev. Lett.* **62**, 2056 (1989).
  - [5] P. Chandra and B. Doucot, *Phys. Rev. B* **38**, 9335 (1988).
  - [6] E. Dagotto and A. Moreo, *Phys. Rev. Lett.* **63**, 2148 (1989).
  - [7] H.J. Schulz and T.A.L. Ziman, *Europhys. Lett.* **18**, 355 (1992); H.J. Schulz, T.A.L. Ziman, and D. Poilblanc, *J. Phys. I* **6**, 675 (1996).
  - [8] J. Richter, *Phys. Rev. B* **47**, 5794 (1993).
  - [9] M.E. Zhitomirsky and K. Ueda, *Phys. Rev. B* **54**, 9007 (1996).
  - [10] R.F. Bishop, D.J.J. Farnell, and J.B. Parkinson, *Phys. Rev. B* **58**, 6394 (1998).
  - [11] R. R. P. Singh, Z. Weihong, C. J. Hamer, and J. Oitmaa, *Phys. Rev. B* **60**, 7278 (1999).
  - [12] L. Capriotti, F. Becca, A. Parola, and S. Sorella, *Phys. Rev. Lett.* **87**, 097201 (2001).
  - [13] J. Sirker, Z. Weihong, O. P. Sushkov, and J. Oitmaa, *Phys. Rev. B* **73**, 184420 (2006).
  - [14] D. Schmalfuß, R. Darradi, J. Richter, J. Schulenburg, and D. Ihle, *Phys. Rev. Lett.* **97**, 157201 (2006).
  - [15] M. Mambrini, A. Läuchli, D. Poilblanc, and F. Mila, *Phys. Rev. B* **74**, 144422 (2006).
  - [16] R.F. Bishop, P.H.Y. Li, R. Darradi, J. Schulenburg and J. Richter, *Phys. Rev. B* **78**, 054412 (2008).
  - [17] R. Darradi, O. Derzhko, R. Zinke, J. Schulenburg, S. E. Krüger, and J. Richter, *Phys. Rev. B* **78**, 214415 (2008).
  - [18] V. Murg, F. Verstraete, and J. I. Cirac, *Phys. Rev. B* **79**, 195119 (2009).
  - [19] J. Richter and J. Schulenburg, *Eur. Phys. J. B* **73**, 117 (2010).
  - [20] J. Reuther and P. Wölfle, *Phys. Rev. B* **81**, 144410 (2010).
  - [21] H.-C. Jiang, H. Yao, and L. Balents, *Phys. Rev. B* **86**, 024424 (2012).

- [22] L. Wang, D. Poilblanc, Z.-C. Gu, X.-G. Wen, F. Verstraete Phys. Rev. Lett. **111**, 037202 (2013).
- [23] W.-J. Hu, F. Becca, A. Parola, and S. Sorella, Phys. Rev. B **88**, 060402 (2013).
- [24] Shou-Shu Gong, Wei Zhu, D. N. Sheng, O. I. Motrunich, M. P. A. Fisher, Phys. Rev. Lett. **113**, 027201 (2014).
- [25] A. Metavitsiadis, D. Sellmann, and S. Eggert, Phys. Rev. B **89**, 241104(R) (2014).
- [26] J. Richter, R. Zinke, D.J.J. Farnell, Eur. Phys. J. B **88**, 2 (2015).
- [27] A.F. Barabanov A.V. Mikheyenkov, N.A. Koslov, Pisma JETP **102**, 333 (2015).
- [28] S. Morita, R. Kaneko, and M. Imada J. Phys. Soc. Japan **84**, 024720 (2015)
- [29] T.P. Cysne and M.B. Silva Neto, Europhys. Lett. **112**, 47002 (2015)
- [30] C.A. Lamas, D.C. Cabra, P. Pujol, and G.L. Rossini, Eur. Phys. J. B **88**, 176 (2015).
- [31] P. Carretta, N. Papinutto, C. B. Azzoni, M. C. Mozzati, E. Pavarini, S. Gonthier, and P. Millet, Phys. Rev. B **66**, 094420 (2002).
- [32] R. Melzi, P. Carretta, A. Lascialfari, M. Mambrini, M. Troyer, P. Millet, and F. Mila, Phys. Rev. Lett. **85**, 1318 (2000); R. Melzi, S. Aldrovandi, F. Tedoldi, P. Carretta, P. Millet, and F. Mila, Phys. Rev. B **64**, 024409 (2001); H. Rosner, R. R. P. Singh, W. H. Zheng, J. Oitmaa, and W. Pickett, Phys. Rev. B **67**, 014416 (2003).
- [33] T. Koga, N. Kurita, H. Tanaka, J. Phys. Soc. Jpn. **83**, 115001 (2014).
- [34] D. Schmalfuß, R. Darradi, J. Richter, J. Schulenburg, and D. Ihle, Phys. Rev. Lett. **97**, 157201 (2006).
- [35] O. Rojas, C. J. Hamer and J. Oitmaa, J. Phys.: Cond. Matter **23**, 4160010 (2011).
- [36] M. Holt, O. P. Sushkov, D. Stanek, and G. S. Uhrig, Phys. Rev. B **83**, 144528 (2011).
- [37] Z. Fan and Q.-L. Jie, Phys. Rev. B **89**, 054418 (2014).
- [38] B. Canals and C. Lacroix, Phys. Rev. Lett. **80**, 2933 (1998).
- [39] R. Schmidt, J. Schulenburg, J. Richter, D.D. and Betts, Phys. Rev. B **66(22)**, 224406 (2002)
- [40] J. Oitmaa and Weihong Zheng, Phys. Rev. B **69**, 064416 (2004).
- [41] K. Majumdar and T. Datta, J. Phys.: Condens. Matter **21**, 406004 (2009).
- [42] M.R. Pantić, D.V. Kapor, S.M. Radosević, and P.M. Mali, Solid State Communications **182**, 55 (2014).
- [43] C. Pinettes and H. T. Diep, J. Appl. Phys., **83**, 6317 (1998).
- [44] P. Müller, J. Richter, A. Hauser, and D. Ihle, Eur. Phys. J. B **88**, 159 (2015)

- [45] J. Richter, P. Müller, A. Lohmann, and H.-J. Schmidt, *Physics Procedia* **75**, 813 (2015)
- [46] K. Kubo and T. Kishi, *J. Phys. Soc. Japan* **60**, 567 (1991).
- [47] T. Kishi and K. Kubo, *Phys. Rev. B* **43**, 10844 (1991).
- [48] V. Y. Irkhin, A. A. Katanin, and M. I. Katsnelson, *J. Phys.: Condens. Matter* **4**, 5227 (1992).
- [49] A. F. Barabanov, V. M. Beresovsky, and E. Zasiwas Phys. Rev. B **52**, 10177 (1995).
- [50] J. R. Viana, J. R. de Sousa, and M. Continentino, *Phys. Rev. B* **77**, 172412 (2008).
- [51] K. Majumdar and T. Datta, *J. Stat. Phys.* **139**, 714 (2010).
- [52] M. Laubach, D. G. Joshi, J. Reuther, R. Thomale, M. Vojta, and S. Rachel, *Phys. Rev. B* **93**, 041106(R) (2016).
- [53] J. Richter, R. Darradi, J. Schulenburg, D.J.J. Farnell, and H. Rosner, *Phys. Rev. B* **81**, 174429 (2010)
- [54] J. Villain, R. Bidaux, J.P. Carton, and R. Conte, *J. Phys.* **41**, 1263 (1980).
- [55] E.F. Shender, *Zh. Eksp. Teor. Fiz.* **83**, 326 (1982); *ibid* *Sov. Phys. JETP* **56**, 178 (1982).
- [56] R.F. Bishop, *Theor. Chim. Acta* **80**, 95 (1991).
- [57] C. Zeng, D. J. J. Farnell, and R. F. Bishop, *J. Stat. Phys.* **90**, 327 (1998).
- [58] R. F. Bishop, in *Microscopic Quantum Many-Body Theories and Their Applications*, edited by J. Navarro and A. Polls, *Lecture Notes in Physics* **510** (Springer, Berlin, 1998), p.1.
- [59] D. J. J. Farnell and R. F. Bishop, in *Quantum Magnetism*, *Lecture Notes in Physics* **645**, edited by U. Schollwöck, J. Richter, D. J. J. Farnell, and R. F. Bishop (Springer, Berlin, 2004), p. 307.
- [60] J. B. Parkinson and D. J. J. Farnell. *An Introduction To Quantum Spin Systems*. *Lecture Notes In Physics* **816**. (Springer Verlag, 2010), p. 109.
- [61] R.F. Bishop, D.J.J. Farnell, S.E. Krüger, J.B. Parkinson, J. Richter and C. Zeng, *J. Phys.: Condens. Matter* **12** 6887 (2000).
- [62] S.E. Krüger, J. Richter, J. Schulenburg, D.J.J. Farnell and R.F. Bishop, *Phys. Rev. B* **61**, 14607 (2000).
- [63] R. Darradi, J. Richter, and D. J. J. Farnell, *Phys. Rev. B* **72**, 104425 (2005).
- [64] R.F. Bishop, P.H.Y. Li, R. Darradi, and J. Richter, *J. Phys.: Condens. Matter* **20**, 255251 (2008).
- [65] O. Götze, D.J.J. Farnell, R.F. Bishop, P.H.Y. Li, and J. Richter, *Phys. Rev. B* **84**, 224428 (2011).

- [66] D.J.J. Farnell, R.F. Bishop, P.H.Y. Li, J. Richter, and C. E. Campbell; Phys. Rev. B **84**, 012403 (2011).
- [67] D.J.J. Farnell, O. Götze, J. Richter, R.F. Bishop, and P.H.Y. Li, Phys. Rev. B **89**, 184407 (2014).
- [68] O. Götze and J. Richter, Phys. Rev. B **91**, 104402 (2015).
- [69] O. Götze and J. Richter, arXiv:1510.04898.
- [70] J.J. Jiang, Y.J. Liu, F. Tang, C.H. Yang, and C.-H. Yang, J. Phys. Soc. Jpn. **84**, 114713 (2015).
- [71] J.J. Jiang, Y.J. Liu, F. Tang, C.H. Yang, Physica B: Condensed Matter **463**, 30 (2015).
- [72] R. F. Bishop, P. H. Y. Li, O. Götze, J. Richter, and C. E. Campbell, Phys. Rev. B **92**, 224434 (2015).
- [73] D.J.J. Farnell, K.A. Gernoth, and R.F. Bishop, J. Stat. Phys. **108**, 401 (2002).
- [74] J. Oitmaa, C.J. Hamer, and Zheng Weihong, Phys. Rev. B **50**, 3877 (1994).
- [75] S.E. Krüger, R. Darradi, J. Richter, and D.J.J. Farnell, Phys. Rev. B **73**, 094404 (2006).
- [76] C. J. Hamer, W. Zheng, and J. Oitmaa, Phys. Rev. B **50**, 6877 (1994).
- [77] T. Einarsson and H. J. Schulz, Phys. Rev. B **51**, R6151 (1995).
- [78] P. Lecheminant, B. Bernu, C. Lhuillier, L. Pierre, Phys. Rev. B **52**, 9162 (1995).
- [79] L. O. Manuel, A. E. Trumper, and H. A. Ceccatto, Phys. Rev. B **57**, 8348 (1998).
- [80] O. Götze, J. Richter, R. Zinke and D. J. J. Farnell, J. Magn. Magn. Mat. **397**, 333 (2016).
- [81] D.J.J. Farnell, J. Richter, R. Zinke, and R.F. Bishop, Journal of Statistical Physics **135**, 175 (2009).
- [82] Y. Xian, J. Phys.: Condens. Matter **6**, 5965 (1994).
- [83] T. Oguchi, H. Nishimori, and Y. Taguchi, J. Phys. Soc. Jpn. **54**, 4494 (1985).